Journal of Magnetism and Magnetic Materials 322 (2010) 2223–2226

Contents lists available at ScienceDirect

Journal of Magnetism and Magnetic Materials

journal homepage: www.elsevier.com/locate/jmmm

Carbon-doping effects on the metamagnetic transition and magnetocaloric effect in $MnAsC_x$

W.B. Cui, W. Liu *, Q. Zhang, B. Li, X.H. Liu, F. Yang, X.G. Zhao, Z.D. Zhang

Shenyang National Laboratory for Materials Science, Institute of Metal Research, International Center for Materials Physics, Chinese Academy of Sciences, Shenyang 110016, People's Republic of China

ARTICLE INFO

Article history:
Received 2 March 2009
Received in revised form
17 December 2010
Available online 13 February 2010

Keywords:
Magneto-caloric effect
Metamagnetic phase transition
Carbon-doping effect

ABSTRACT

Carbon doping effects in MnAs alloys have been investigated. More carbon doping in MnAs alloys leads to lower Curie temperature, larger thermal hysteresis and sharper slope of the dependence of critical field on reduced temperature due to severe lattice distortion. The obtained maximum of magnetic entropy change for a field change of 5 T is about 12.8 J kg^{-1} K^{-1} near room temperature, and increases with more doping carbon content to about 22.4 J kg^{-1} K^{-1} in $MnAsC_{0.03}$ and 13.2 J $kg^{-1}K^{-1}$ in $MnAsC_{0.05}$.

1. Introduction

Recently, much interest has been focused on using the magnetocaloric effect (MCE) as an alternate technology for refrigeration, in order to replace common gas-compression/expansion technology, due to efficiency and environmental concerns [1]. In particular, room-temperature magnetic refrigeration materials have been of much concern [2–5]. In order to realize this purpose, it is important to explore the compounds with large entropy changes near room temperature. Conventional MCE is observed for materials with second-order magnetic transitions and the MCE would be much increased when the transition is of first-order phase transition [6–8]. There is also a first-order phase transition in MnAs under hydrostatic pressure [8]. When subjected to pressure, similar large MCE was found in $Gd_5Ge_2Si_2$ [9], $La_{0.8}Sr_{0.2}MnO_3$ [10] and $La(Fe_{1-x}Si_x)_{13}H_y$ [11] assisted by magnetoelastic interactions. Specifically, bulk MnAs undergoes a magnetic transition from a ferromagnetic (FM) phase to a paramagnetic (PM) phase at T_c=313 K, accompanied by a structural transition from hexagonal NiAs-type to orthorhombic MnP-type [12]. The phase transition is strongly sensitive to the pressure caused by lattice distortion [8]. The substitution effect of 3d elements, which is considered to mimic the role of pressure, has been extensively investigated [13–15]. However, introducing interstitial atoms with small radius can also play the role of pressure. Interstitial effects of carbon [16] and hydrogen [11,17] in La–Fe–Si system and boron in Ni–Mn–Sn system [18] have been investigated. To date, nearly all investigations focused on substitution effects on MCE in MnAs system. In this paper, interstitial effects of carbon doping on the phase transition and MCE in the MnAs system are investigated. It is found that carbon doping can lead to lower Curie temperature, increased thermal hysteresis and sharper slope of dependence of critical field on reduced temperature. The maximum of magnetic entropy change for the field change of 5 T decreases with increase in carbon doping.

2. Experiments

Polycrystalline $MnAsC_x$ compounds (x=0, 0.015, 0.03 and 0.5) were synthesized by mechanical alloying, which was developed to avoid the volatilization of As and time-exhausting solid-state reaction. Powders of Mn, As and C with purity more than 99.9% were mixed according to the nominal compositions. The mixtures of 10 g were sealed in hardened steel vials with steel balls of 12 mm diameter in a high purity argon filled glove box. Mechanical alloying was carried out for 5 h using a high-energy ball mill that was rotated in two dimensions perpendicular to the horizontal plane [13]. The rotation speed of the mill was chosen to be 800 rpm. The weight ratio of ball-to-powder was 30:1. The mechanically alloyed powders were annealed at 773 K for 2 h and then elevated to 973 K for another 2 h in vacuum more than 10^{-3} Pa. X-ray diffraction (XRD) analysis was conducted using CuKα radiation with a Rigaku D/Max-γA diffractometer equipped with a graphite crystal monochromator. The magnetic properties were measured using a superconducting quantum interference device (SQUID) with fields up to 5 T. The change of magnetic

* Corresponding author. Fax: +86 24 23891320.
E-mail address: wliu@imr.ac.cn (W. Liu).

0304-8853/$ - see front matter © 2010 Elsevier B.V. All rights reserved.
doi:10.1016/j.jmmm.2010.02.014

entropy was calculated from M–B plots close to their respective Curie temperature (T_c).

3. Results and discussions

All XRD patterns of $MnAsC_x$ (x=0.015, 0.03 and 0.05) alloys show the MnP-type orthorhombic structure at room temperature. Fig. 1 shows the thermo-magnetic M–T curves for $MnAsC_x$ (x=0.015, 0.03 and 0.05) under 0.01 T on cooling and heating processes. A sharp decrement is observed on magnetization near Curie temperatures, which are all below 295 K, meaning a phase transition from a NiAs-type ferromagnetic (FM) state to MnP-type paramagnetic (PM) state. More carbon addition leads to the decrease of T_c from 280 K in $MnAsC_{0.015}$ to 277 K in $MnAsC_{0.03}$ and 256 K in $MnAsC_{0.05}$ for a heating process. However, the presence of thermal hysteresis indicates the first-order nature of the phase transition. It can be seen that the thermal hysteresis is extended with more carbon addition, indicating that enlarged potential barrier is necessary to induce phase transition. Because the phase transitions in MnAs-based alloys are of first-order structural transition, the lattice distortion caused by increase in carbon content would influence the structural transition as reported in Refs. [11,16–18] and be responsible for the extended thermal hysteresis.

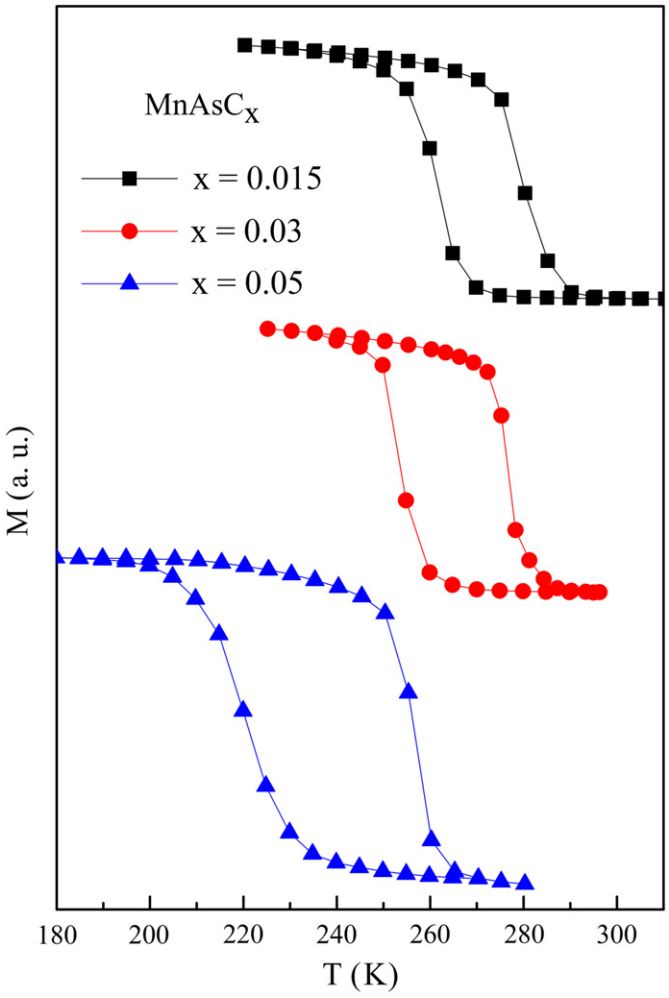

Fig. 1. Temperature dependence of magnetization curves for $MnAsC_x$ (x=0.015, 0.03 and 0.05) under 0.01 T on cooling and heating processes.

To make clear the influence of the external field on the structural transition and MCE in $MnAsC_x$, isothermal magnetization $M(B)$ curves are recorded near their Curie temperature in a heating process (see Fig. 2). It can be seen that magnetization increases rapidly and shows a tendency to saturate at a low field at 272 and 275 K, indicating an FM state with NiAs-type structure in $MnAsC_{0.015}$. With increase in temperature, an abrupt increment is observed on the isothermal magnetization process, revealing a field-induced metamagnetic transition, accompanied by a structural transition from orthorhombic MnP-type to hexagonal NiAs-type [8]. Similar stepwise behaviors also appear on the M–B curves at different temperature for other carbon-doped MnAs alloys. With increase in temperature, the occurrence of metamagnetic transition moves to higher field.

Fig. 3 gives the dependence of critical fields (B_{cr}) to induce the metamagnetic transition on the reduced temperature (t) for $MnAsC_x$ (x=0.015 and 0.03). It can be seen from Fig. 2(c) that the occurrence of metamagnetic transition in $MnAsC_{0.05}$ is greatly postponed to more than 5 T, the dependence of B_{cr} on the reduced temperature in $MnAsC_{0.05}$ is not shown in Fig. 3. Additionally, the slope of B_{cr}–t curve seems sharper for $MnAsC_{0.03}$ than that of $MnAsC_{0.015}$. More carbon doping content leads to severe lattice distortion and larger Gibbs energy barrier between two phases, which needs higher magnetic field to overcome Gibbs energy barrier to induce the magnetic transitions accompanied with the structural transition. Therefore, steeper slopes of B_{cr}–t curves are observed.

The magnetic entropy change is usually calculated by the Maxwell relationship $\Delta S_M(T) = \int_0^B (\partial M/\partial T)_B dB$. The calculated temperature dependences of $\Delta S_M(T)$ for $MnAsC_x$ (x=0.015, 0.03 and 0.05) under a field change of 5 T are shown in Fig. 4. It is argued that in the first-order phase transformation the magnetic entropy change calculated from Maxwell relationship (MR) is significantly different from the real value, especially in the region of phase transformation, where an abnormal "spike" would be observed. Such deviation is mainly because of incorrectly neglecting the co-existence of paramagnetic phase and ferromagnetic phase. Some improvements have been made on the calculation of magnetic entropy change [19,20]. Generally, in the first-order phase transition, the Clausius–Clapeyron (CC) equation is more accurate in determining the magnetic entropy change, especially in the region of phase transition [21]. Here, because the magnetization is not fully saturated in our system, the real magnetic entropy change is calculated by considering the co-existence of paramagnetic and ferromagnetic phases [19], as shown in Fig. 4, in comparison with the results calculated directly by the Maxwell relationship. It can be seen that magnetic entropy change increases from 12.8 J kg^{-1} K^{-1} at x=0.015 to 22.4 J kg^{-1} K^{-1} at x=0.03 and then decreases to 13.2 J kg^{-1} K^{-1} at x=0.05, all of which are much lower than the corresponding nominal magnetic entropy change calculated by the Maxwell relationship. Since Wada and Tanabe [3] reported the large magnetocaloric effect in MnAs system, much work has been done on the substitution effects in MnAs systems [12–15,20,22,23]. However, the interstitial effects in MnAs system are investigated in the present paper. So it would be interesting to compare the substitutional and interstitial effect on the ΔS_M, T_c and thermal hysteresis in MnAs based alloys, as listed in Table 1. From Table 1, it can be seen that the thermal hysteresis in MnAs system can be reduced to nearly zero only by Cr substitution for Mn and Si substitution for As. The accompanied phase transition is more like a second-order one, with obscure or even no inflexion point on the isothermal magnetization curves. The magnetic entropy changes in MnAs based compound in Table 1 range from 20 to 30 J kg^{-1} K^{-1}, except in $Mn_{1-x}Cu_xAs$ system where ΔS_M is directly obtained by Maxwell relationship. However, if we ignore

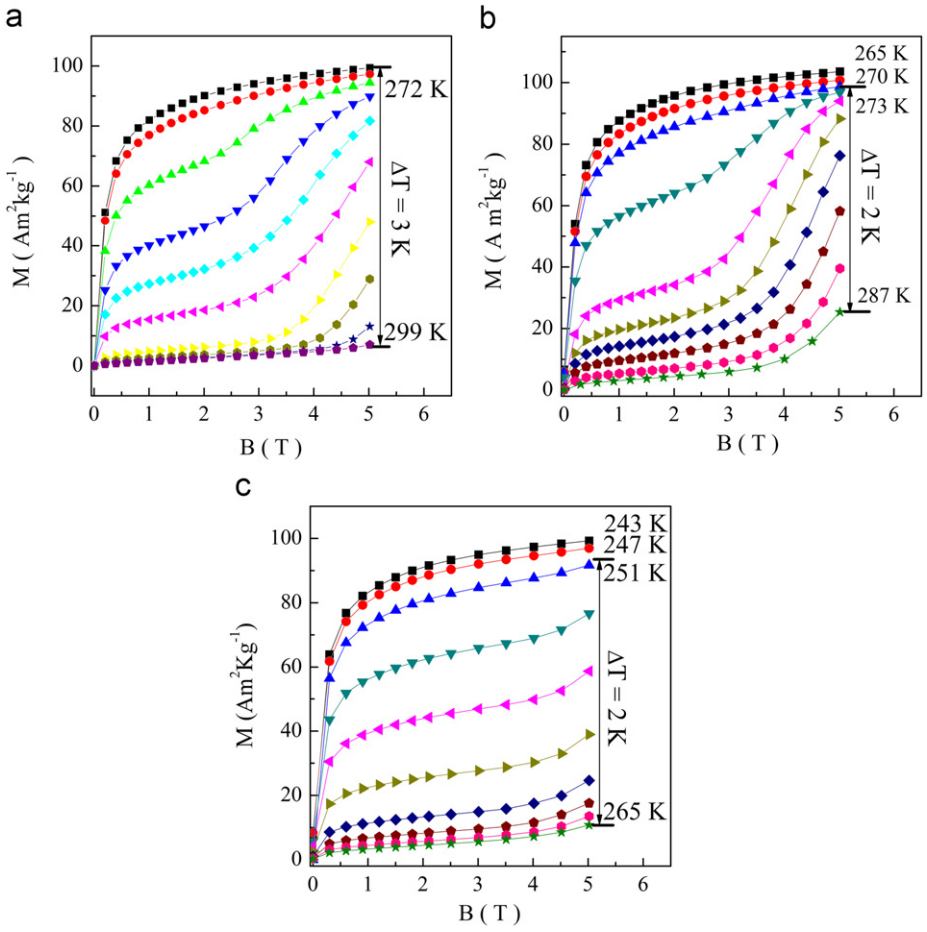

Fig. 2. Isothermal magnetization curves near their respective Curie temperature under magnetic field from 0 to 5 T for (a) $MnAsC_{0.015}$, (b) $MnAsC_{0.03}$ and (c) $MnAsC_{0.05}$. The measurements were carried out with increasing temperature.

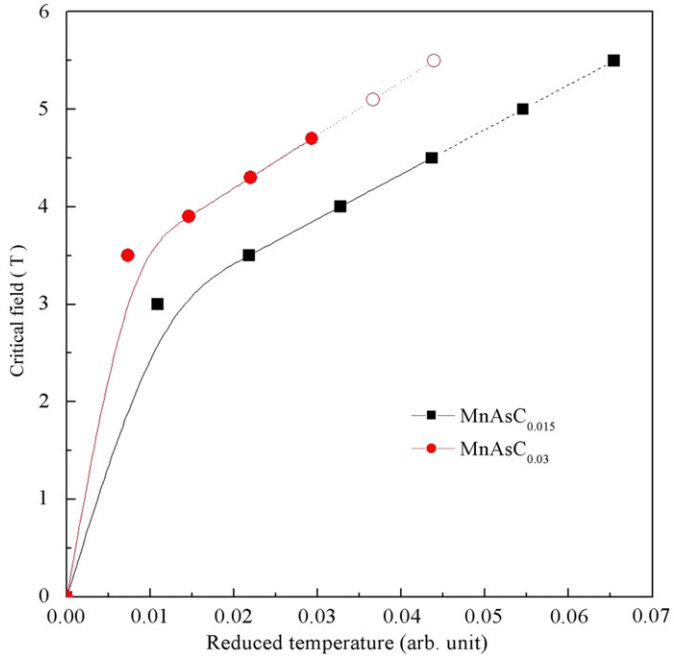

Fig. 3. Dependence of critical field (B_{cr}) on the reduced temperature for $MnAsC_x$ (x=0.015 and 0.03). The closed and open symbols represent real and estimated critical field.

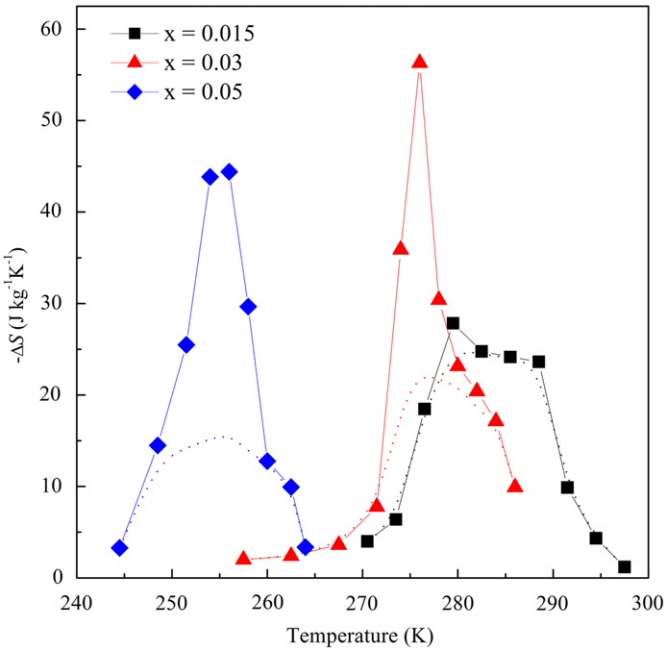

Fig. 4. Magnetic entropy changes as the function of temperature and carbon content under a magnetic field change of 5 T (the solid lines). The dashed line shows the estimated value of magnetic entropy change considering the co-existence of paramagnetic and paramagnetic phases and the calculation of the estimated values could be referred in Ref. [19].

Table 1
Comparison of some main parameters in MnAs based systems.

	ΔS (J kg^{-1} K^{-1})	T_c (in heating process)	Thermal hysteresis	Reference
$MnAs_{1-x}Sb_x$	32 (x=0) (B_{max}=5 T)	318 K (x=0)–230 K (x=0.25)	5 K (x=0)–0 K($x \geq 0.05$)	Ref. [3]
$Mn_{1-x}Fe_xAs$	26 (x=0.01) (B_{max}=5 T) Ref. [20]	320 K (x=0)–280 K (x=0.015) Ref. [15]	10 K (x=0)–28 K (x=0.015) (B=0.02 T) Ref. [15]	
$Mn_{1-x}Cu_xAs$	45–175 (x=0.02, peak value) (B_{max}=5 T)	317 K–323 K	12 K (x=0.003)–20 K (x=0.02) (B=0.02 T)	Ref. [15]
$Mn_{1-x}Cr_xAs$	13 (x=0.01)–20 (x=0.006) (B_{max}=5 T)	265 K (x=0.01)–290 K (x=0.006)	$\approx$0 K (x=0.006)–3 K (x=0.01) (B=0.01 T)	Ref. [13]
$Mn_{1-x}(Ti_{0.5}V_{0.5})_xAs$	$\approx$30 (x=0.1) (B_{max}=2 T)	318 K (x=0)–266 K (x=0.1)		Ref. [22]
$MnAs_{1-x}Si_x$	14 (x=0.03)–10.9 (x=0.09) (B_{max}=5 T)	270 K (x=0.03)–297 K (x=0.09)	5 K (x=0.03)–$\approx$0 K (x=0.09) (B=0.01 T)	Ref. [23]
$MnAsC_x$	12.8 (x=0.015)–22.4 (x=0.03) (B_{max}=5 T)	280 K (x=0.015)–256 K (x=0.05)	18 K (x=0.015)–35 K (x=0.05) (B=0.01 T)	Present work

the "spike" value in the phase transition region in $Mn_{1-x}Cu_xAs$ system, the magnetic entropy values in the plateau region in ΔS_M–T curves still range from 20 to 30 J kg^{-1} K^{-1}, which may be the reasonable value for MnAs based compound.

4. Conclusions

In conclusion, carbon-doping effects in MnAs alloys are investigated. Curie temperature decreases from 280 K in $MnAsC_{0.015}$ to 256 K in $MnAsC_{0.03}$. Larger thermal hysteresis and sharper slope of B_{cr}–t with more carbon content are observed, which may be due to the severe lattice distortion. For a field change of 5 T, maximum of magnetic entropy change in $MnAsC_{0.015}$ is about 12.8 J kg^{-1} K^{-1} near room temperature. More doping carbon content leads to about 22.4 J kg^{-1} K^{-1} in $MnAsC_{0.03}$ and 13.2 J kg^{-1} K^{-1} in $MnAsC_{0.05}$.

Acknowledgements

This work has been supported by the National Nature Science Foundation of China under Projects 50831006 and 50971123 and National Basic Research Program (No. 2010CB934603) of China, the Ministry of Science and Technology of China.

References

[1] C.B. Zimm, A. Jastrab, A. Sternberg, V.K. Pecharsky, K.A. Gschneidner Jr., M. Osborne, I. Anderson, Adv. Cryog. Eng. 43 (1998) 1759.
[2] O. Tegus, E. Brück, K.H.J. Buschow, F.R. de Boer, Nature 415 (2002) 150.
[3] H. Wada, Y. Tanabe, Appl. Phys. Lett. 79 (2001) 3302.
[4] A. Fujita, S. Fujieda, K. Fukamichi, H. Mitamura, T. Goto, Phys. Rev. B 65 (2001) 014410.
[5] S. Yu Dan' kov, A.M. Tishin, V.K. Pecharsky, K.A. Gschneidner Jr., Phys. Rev. B 57 (1998) 3478.
[6] K.A. Gschneidner Jr., V.K. Pecharsky, A.O. Tsokol, Rep. Prog. Phys. 68 (2005) 1479.
[7] E. Brück, J. Phys. D 38 (2005) R381.
[8] S. Gama, A.A. Coelho, A. de Compos, A.M.G. Carvalho, F.C.G. Gandra, P.J. von Ranke, N.A. de Oliveria, Phys. Rev. Lett. 93 (2004) 237202.
[9] A.M.G. Carvalho, C.S. Alves, A. de Campos, A.A. Coelho, S. Gama, F.C.G. Gandra, P.J. von Ranke, N.A. de Oliveira, J. Appl. Phys. 97 (2005) 10M320.
[10] D.L. Rocco, R.A. Silva, A.M.G. Carvalho, A.A. Coelho, J.P. Andreeta, S. Gama, J. Appl. Phys. 97 (2005) 10M317.
[11] Young Sun, Z. Arnold, J. Kamarad, Guang-Jun Wang, Bao-Geng Shen, Zhao-Hua Cheng, Appl. Phys. Lett. 89 (2006) 172513.
[12] J. Mira, F. Rivadulla, J. Rivas, A. Fondado, T. Guidi, R. Caciuffo, F. Carsughi, P.G. Radaelli, J.B. Goodenough, Phys. Rev. Lett. 90 (2003) 097203.
[13] N.K. Sun, W.B. Cui, D. Li, D.Y. Geng, F. Yang, Z.D. Zhang, Appl. Phys. Lett. 92 (2008) 072504.
[14] A. de Campos, D.L. Rocco, A.M.G. Carvalho, L. Caron, A.A. Coelho, S. Gama, L. da Silva, F.C.G. Gandra, A. O dos Santos, L.P. Cardoso, P.J. von Ranke, N.A. de Oliveira, Nat. Mater. 5 (2006) 802.
[15] D.L. Rocco, A. de Campos, A.M.G. Carvalho, L. Caron, A.A. Coelho, S. Gama, F.C.G. Gandra, A. O dos Santos, L.P. Cardoso, P.J. von Ranke, N.A. de Oliveira, Appl. Phys. Lett. 90 (2007) 242507.
[16] Yuan-fu Chen, Fang Wang, Bao-gen Shen, Guang-jun Wang, Ji-rong Sun, J. Appl. Phys. 93 (2003) 1323.
[17] K. Mandal, D. Pal, O. Gutfleisch, P. Kerschl, K.H. Müller, J. Appl. Phys. 102 (2007) 053906.
[18] H.C. Xuan, D.H. Wang, C.L. Zhang, Z.D. Han, B.X. Gu, Y.W. Du, Appl. Phys. Lett. 92 (2008) 102503.
[19] G.J. Liu, J.R. Sun, J. Shen, B. Gao, H.W. Zhang, F.X. Hu, B.G. Shen, Appl. Phys. Lett. 90 (2007) 032507.
[20] M. Balli, D. Fruchart, D. Gignoux, R. Zach, Appl. Phys. Lett. 95 (2009) 072509.
[21] A. Giguère, M. Földeaki, B. Ravi Goopal, R. Chahine, T.K. Bose, A. Frydman, J.A. Barcley, Phys. Rev. Lett. 83 (1999) 2262.
[22] M. Balli, D. Fruchart, D. Gignoux, C. Dupuis, A. Kedous-Lebouc, R. Zach, J. Appl. Phys. 103 (2008) 103908.
[23] W.B. Cui, W. Liu, X.H. Liu, S. Guo, Z. Han, X.G. Zhao, Z.D. Zhang, J. Alloys Compd. 479 (2009) 189.